GNSS Signal Primer

Global Navigation Satellite Systems (GNSS) embed their navigation data—augmented with forward-error-correction and pilot channels—onto narrowband carriers using Binary Phase-Shift Keying (BPSK). Each satellite then "spreads" that power across a much wider bandwidth (on the order of a few MHz) via Direct-Sequence Spread Spectrum (DSSS). This DS-CDMA approach:

1. Improves ranging accuracy, since correlation process yields processing gain
2. Enhances multipath resilience, by decorrelating delayed echoes
3. Mitigates narrowband interference, by distributing interfering tones across the full spread band

Every satellite has its own pseudo-noise (PRN) code, so multiple satellites can share the same RF band without mutual interference. On top of the basic BPSK-DSSS, many modern GNSS signals layer on Binary Offset Carrier (BOC) and Composite BOC (CBOC/TMBOC) waveforms to further shape their spectrum and improve robustness.

In the paragraphs below, we present a consolidated analytical overview of GNSS baseband signal structures—focusing on the two largest constellations, GPS and Galileo. Our goal is to give a unified set of equations that shows exactly how:

- Ranging codes (c(t))
- Navigation data (d(t)) and,
- Carrier/sub-carrier modulation (BPSK, BOC, CBOC)

combine in each system.

We include the official, ICD-mandated expressions for GPS L1 C/A, L1 P(Y), L2C, L5, and Galileo E1 OS, E5a, E5b, E6.

Supplementary or configuration-specific variants (e.g. pilot-only channels, encrypted military codes) are noted but not listed in full—since they follow directly by toggling data vs. pilot or swapping PRN sequences.

1. BPSK-DSSS Baseband Model

The simplest GNSS waveform is plain BPSK-DSSS. In baseband form it reads:

$$s_{BPSK}(t) = \alpha\, c(t)\, d(t)$$

where α sets the overall signal power, $c(t)$ is the PRN code (±1 at the chip rate), $d(t)$ is the navigation data (±1 at the bit rate).

The legacy GPS L1 C/A signal carries one PRN code and one data stream, both at 1.023 Mcps:

$$x_{L1CA}(t) = c_{L1CA}(t)\, d_{L1CA}(t)$$

where both $c_{L1CA}(t)$ and $d_{L1CA}(t)$ take values ±1. This structure yields a processing gain of approximately 43 dB, derived from a chip rate of 1.023 Mcps and a data rate of 50 bps.

The power spectral density of L1 C/A signal as an example of BPSK modulated signal spectrum is given in Figure 1, and will be detailed in Section 4 of this paper.

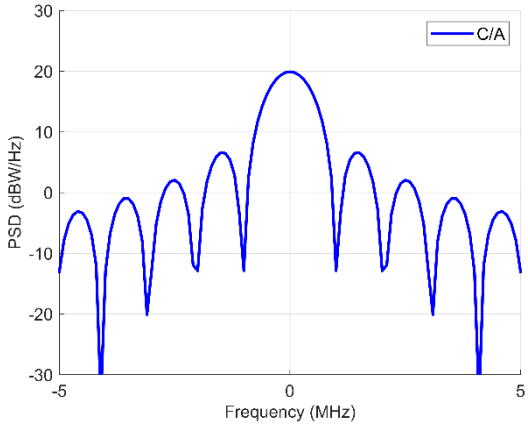

Figure 1. Power Spectral Density of GPS L1 C/A Signal Normalized to 1-Watt.

Since L5 uses two orthogonal PRN codes, one on the in-phase branch and one on the quadrature branch, its baseband is complex:

$$x_{L5}(t) = c_{L5I}(t)\, d_{L5}(t) + j\, c_{L5Q}(t)$$

The real part carries the I-code and data while the imaginary part carries the Q-code (typically pilot-only).

Thanks to its 10.23 Mcps spreading and 100 bps data rate, the L5 waveform achieves a processing gain of 50 dB, enhancing resistance to interference and multipath.
Figure 2 depicts the L5 I- and Q-code spectrums.

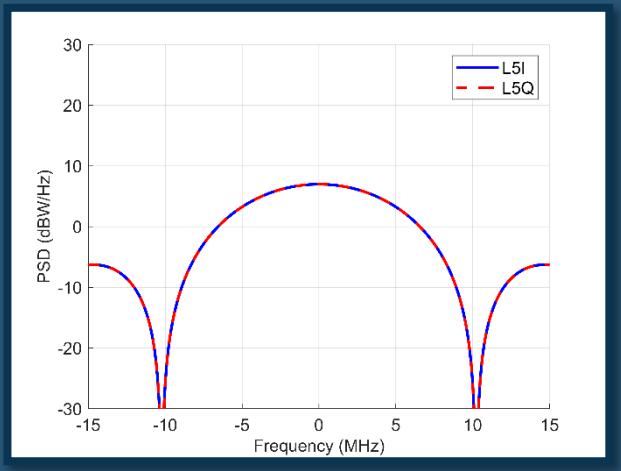

Figure 2. Power Spectral Density of GPS L5 I-code and Q-Code Signals Normalized to 1-Watt

2. Binary Offset Carrier (BOC)

A pure BPSK spectrum is centered at the carrier. BOC shifts most of the energy away from the center by multiplying by a ±1 sub-carrier:

$$BOC(n,m):\ f_r = m \cdot 1.023\ MHz,$$
$$f_b = n \cdot 1.023\ MHz$$

Depending on phase, the subcarrier is

$$x_{BOC_{S,}\,f_b}(t) = sign(\sin(2\pi f_b t))$$
$$x_{BOC_{c,}\,f_b}(t) = sign(\cos(2\pi f_b t))$$

where BOC_s is sine-phased and BOC_c is cosine-phased. In Figures 3 and 4, we plot the $BOC(10,1)$ sub-carrier as a ±1 square wave over two PRN chips. The x-axis is in units of the BOC symbol period, i.e. one sub-carrier interval of T_{sym}, where

$$T_{sym} = \frac{1\ ms}{10} = 0.1\ ms.$$

Because the sub-carrier is a square wave with 50% duty cycle, each +1 level only lasts for half of the symbol period (the positive half of the underlying sine), and the –1 level occupies the other half. Since BOC(10,1) toggles ten times per chip, a full chip spans 0 to 10 on this normalized axis.

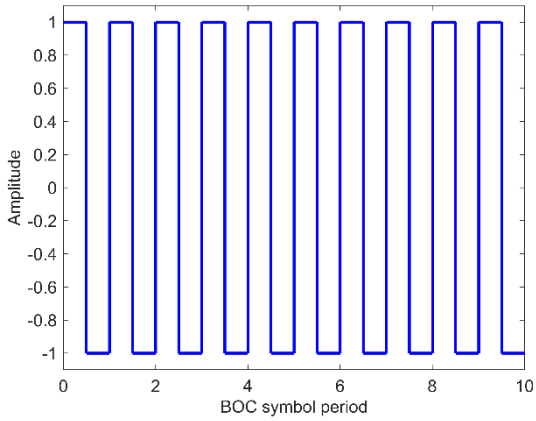

Figure 3. Cosine-Phased BOC

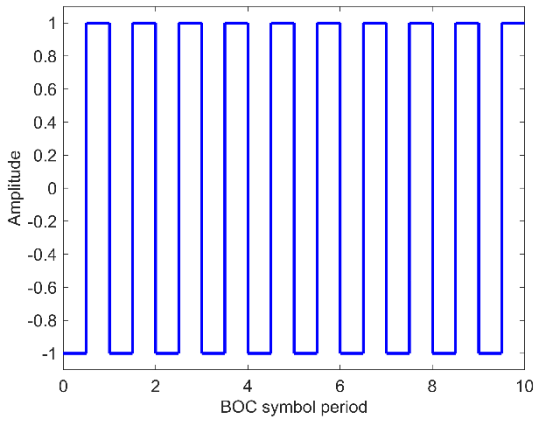

Figure 4. Sine-Phased BOC

For instance, GPS M uses $BOC_s(10,5)$, GALILEO E1 OS uses a composite of $BOC_s(1,1)$ and $BOC_s(6,1)$ that is called $CBOC(6,1,1/11)$. Similarly, L1C data channel uses standard $BOC_s(1,1)$. The power spectral density of L1C data channel as an example of $BOC_s(1,1)$ modulated signal spectrum is given in Figure 5, and will be detailed in Section 4 of this paper.

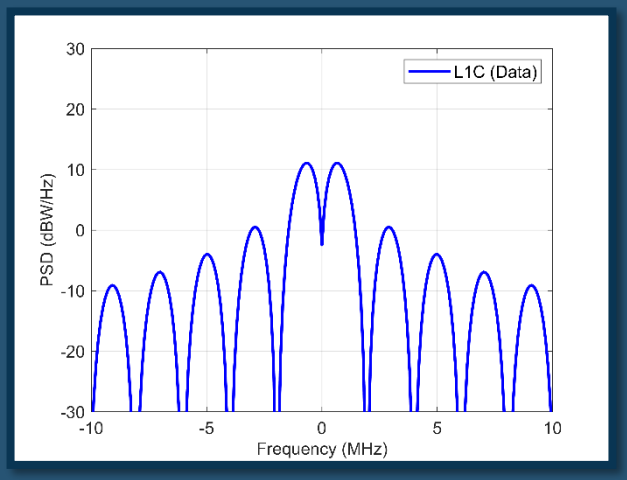

Figure 5. Power Spectral Density of GPS L1C Data Signal Normalized to 1-Watt

3. Composite and Time Multiplexed BOC

Even finer spectral control is achieved by composite and time-multiplexed BOC.

3.1. CBOC (Composite BOC)

Mix a wide- and narrow-subcarrier BOC in fixed power ratio:

$$CBOC\left(\frac{6,1,1}{11}\right) = \sqrt{\frac{10}{11}}BOC_s(6,1) + \sqrt{\frac{1}{11}}BOC_s(1,1)$$

This is what Galileo E1 adopted. Galileo E1 splits into two orthogonal branches—E1B (data) and E1C (pilot)—each constructed from 6.138 MHz and 1.023 MHz sub-carriers. In both plots below, the horizontal axis is in BOC symbol periods, where one period

$$T_b = \frac{1}{f_b} = \frac{1}{1.023\ MHz} = 0.977\ us$$

Figure 6 shows the first 6 symbols of the Galileo E1B sub-carrier. Each toggle from +1 to –1 (or vice versa) spans 0.977 µs; x = 2 corresponds to ~1.95 µs, x = 3 to ~2.93 µs, etc. We truncate at 6 symbols purely for visual clarity—the full PRN repeats every 4092 chips (4 ms).

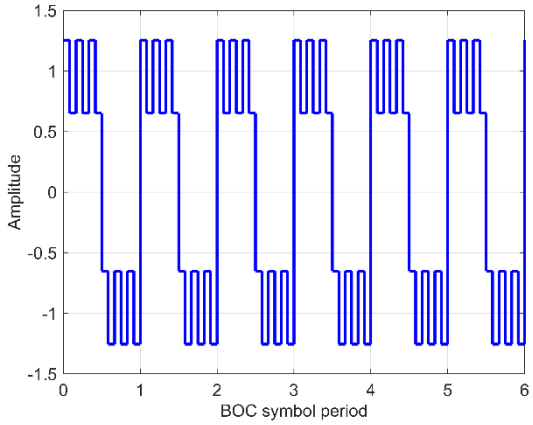

Figure 6. Galileo E1B Sub-Carrier

Figure 7 plots the first 6 symbols (≈5.86 µs) of the pilot component, formed by $-BOC_s(6,1) + BOC_s(1,1)$. The same 0.977 µs symbol period applies. The same 0.977 µs symbol period applies. Again, showing just a few symbols makes the waveform structure visible; over the full 4 ms period, the rapid toggles blend into a continuous sub-carrier.

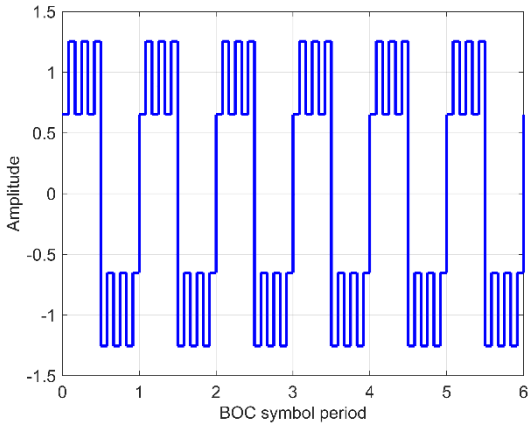

Figure 7. Galileo E1C Sub-Carrier

3.2. TMBOC (Time-Multiplexed BOC)

Alternate blocks of narrow and wide BOC in time:

$$CBOC\left(\frac{6,1,4}{33}\right) = \frac{29}{33}BOC_s(1,1) + \frac{4}{33}BOC_s(6,1)$$

GPS L1 C (the modernized civilian signal) pilot channel, shown in Figure 8, is an example of a TMBOC-modulated signal.

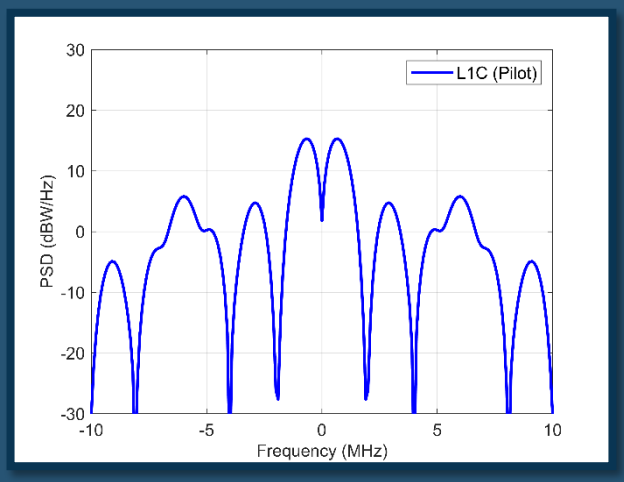

Figure 8. Power Spectral Density of GPS L1C Pilot Signal Normalized to 1-Watt

3.3. AltBOC

Uses two complex sub-carriers instead of one real one to maintain a constant envelope. Internally it can be seen as two QPSK streams at staggered frequencies.

Galileo's E5 AltBOC waveform knits together four real sub-carriers—two "wide" 6.138 MHz components and two "narrow" 1.023 MHz components—into a single constant-envelope signal. Each branch (data or pilot) is built from an eight-chip weight pattern ({a,b,e,f} for data, {d,b,e,c} for pilot) that guarantees the 10:6 power split mandated by the ICD, where

$$\{a,b,e,f\} = \{\frac{\sqrt{2}+1}{2}, \frac{1}{2}, -\frac{1}{2}, -\frac{\sqrt{2}+1}{2}\}$$

$$\{d,c\} = \{-\frac{\sqrt{2}-1}{2}, \frac{\sqrt{2}-1}{2}\}$$

One copy of each weighted pattern is delayed by exactly one PRN-chip period, producing two interleaved sequences per branch. When plotted against "BOC symbol periods" (one period ≃0.977 μs), you can clearly see the ±1 square-wave toggles and how the wide and narrow lobes weave together to shape a spectrum with broad main lobes for fine ranging and deep center notches for interference rejection. Figures 9 and 10 illustrate this for the data and pilot branches, respectively.

In Figure 9, the blue trace is the primary data sub-carrier (E5a-I) at ±1 toggles every symbol period, and the red trace is its delayed counterpart (E5b-I), which smooths the composite envelope.

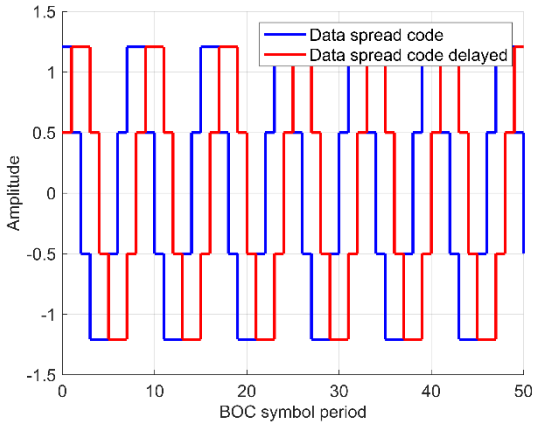

Figure 9. Data Branch of the E5 Altboc Sub-carrier: The Blue Trace Is the Primary Data Channel (E5a-i). The Red Trace Is the Secondary Data Channel (E5b-i), Delayed by One Chip Period.

Figure 10 shows the pilot branch in the same format (E5a-Q in blue, E5b-Q in red), but carrying no navigation bits—allowing the receiver to integrate coherently over much longer intervals for ultra-stable tracking. Together, these four interlaced sequences form the AltBOC(15,2.5) signal that gives E5 its unique blend of precision and robustness.

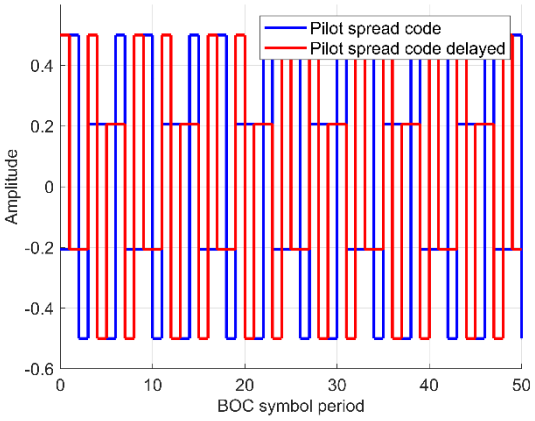

Figure 10. Pilot Branch of the E5 Altboc Sub-carrier: The Blue Trace Is the Primary Pilot Channel (E5a-q). The Red Trace Is the Secondary Pilot Channel (E5b-q), Likewise Delayed by One Chip Period.

Figure 11 plots the full Galileo E5 AltBOC spectrum. Both I (blue) and Q (red) branches occupy ~50 MHz of bandwidth.

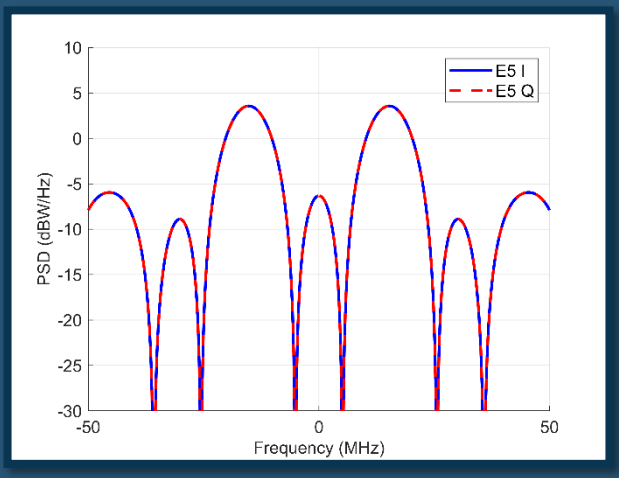

Figure 11. Galileo E5 AltBoc Spectrum

4. Spectral Characteristics of GNSS Signals

To complement our time-domain discussion, in Figures 12–18 below we plot the theoretical power-spectral densities of the major GPS and Galileo signals, computed over a ±50 MHz baseband. Note that each plot is normalized to one watt. Figure 12 shows the legacy GPS L1 spectrum (pre-modernization). The red trace is the in-phase branch (P + M codes), the cyan trace is the quadrature C/A branch, and the dark blue "composite" curve is their sum.

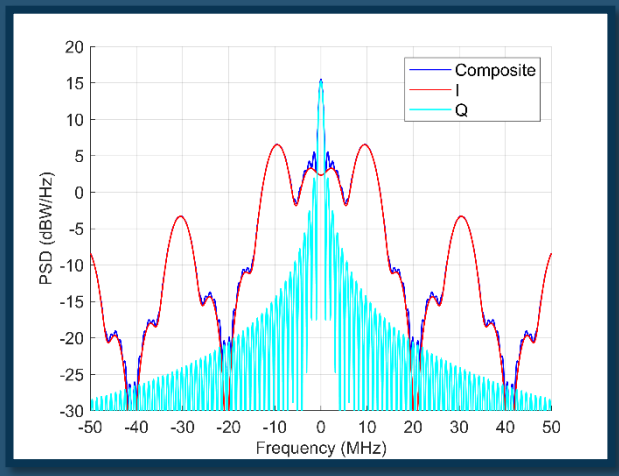

Figure 12. GPS L1 Spectrum

Note the wide ±10 MHz lobes from the P/M sine-phased BOC(10,5) and the narrow central lobe from the BPSK(1.023 MHz) C/A code in Figure 12.

Figure 13 isolates the modernized L1C signal. Here the data component (blue) and pilot component (red) both employ BOC(1,1) + BOC(6,1) sub-carriers—resulting in the interleaved series of side-lobes clustered around ±1.023 MHz.

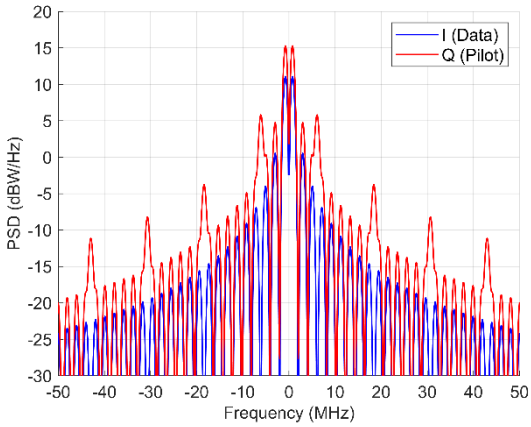

Figure 13. L1C Spectrum

Figure 14 overlays all four Block III L1 components—C/A (blue), P-code (red), M-code (cyan), and L1C (black)—each normalized to one watt. One can clearly see how each modulation contributes its own lobe structure, yet the total remains spectrally compact.

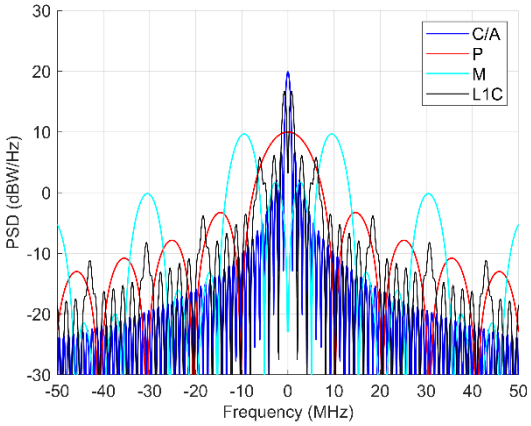

Figure 14. L1 Block III Components Spectra

Figure 15 directly compares the composite spectra before and after Block III. The red curve (Block III) shows slightly deeper notches at ±10 MHz and a modest reshaping of the central peak—evidence of the new civil L1C carving out additional nulls for interference mitigation.

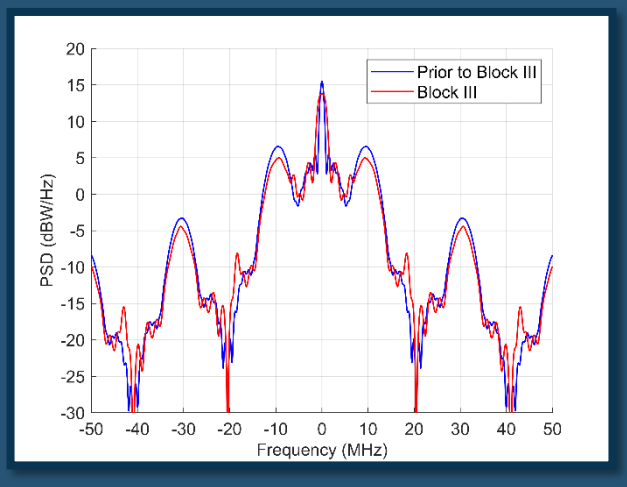

Figure 15. L1 Spectrum Comparison

Figure 16 presents the Galileo E1 band: the OS data branch (blue) uses cosine-phased BOC(15,2.5), yielding narrow ±1.023 MHz lobes, while the PRS pilot branch (red) uses sine-phased BOC(15,2.5), producing wider ±7.5 MHz lobes. Together they span roughly 20 MHz.

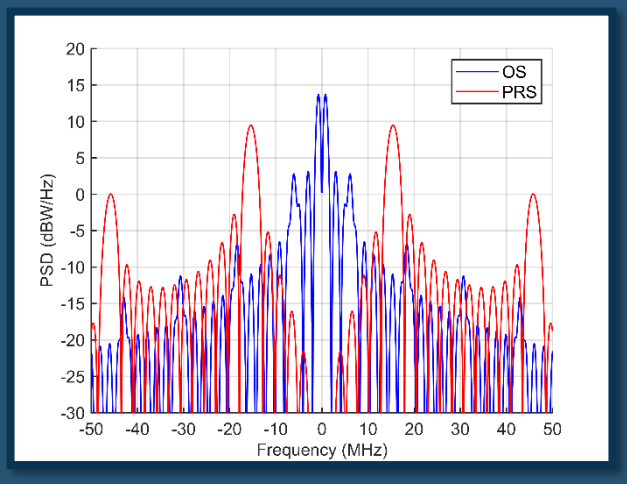

Figure 16. Galileo E1 Spectrum

Figure 17 shows the Galileo E6 band: again the blue OS branch is BOCc(10,5) (±5.115 MHz lobes) and the red PRS branch is BOCs(10,5) (±5.115 MHz lobes inverted), yielding the characteristic cosine- vs. sine-phased spectra.

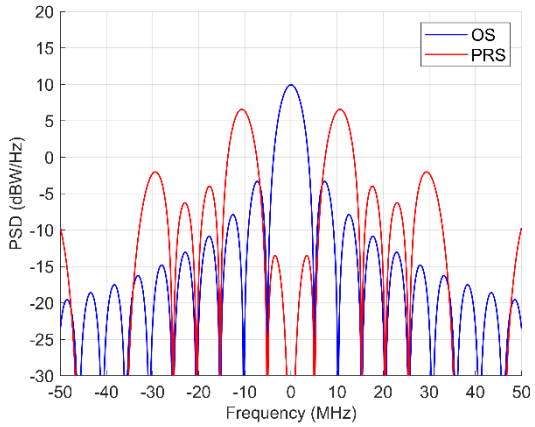

Figure 17. Galileo E6 Spectrum

Finally, Figure 18 zooms in on the E5A half of AltBOC, showing its narrower ~30 MHz span and a single central notch—useful when only the E5A component is tracked.

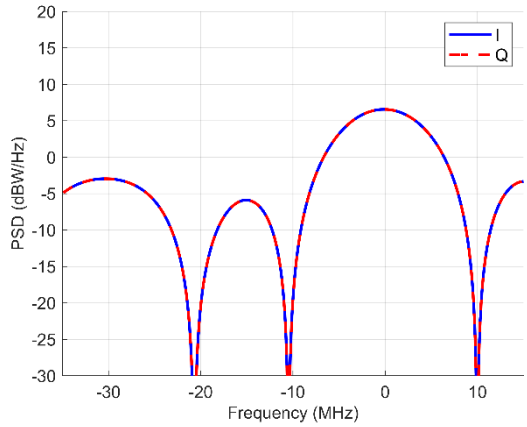

Figure 18. Galileo E5A Half of AltBoc Spectrum

CONCLUSION

In this work, we have developed a unified framework for generating, visualizing, and interpreting modern GNSS waveforms, spanning classic BPSK through diverse BOC variants to the advanced AltBOC hybrid format. Our signal-generation routines faithfully reconstruct the pseudo-noise and sub carrier patterns defined in official interface control documents, and our analytical spectra corroborate the expected main lobe widths, notch depths, and power splits for GPS L1 (legacy and modernized), Galileo E1/E6, and the wide band E5 AltBOC signals.

Our emphasis on the E5 AltBOC format revealed how its eight chip amplitude weights and interleaved data and pilot channels achieve superior timing precision and inherent resistance to narrowband interference. The measured ~50 MHz bandwidth and pronounced spectral nulls at specific offsets confirm AltBOC's design goal of combining high-resolution ranging with built in notch filtering—all without expanding the occupied spectrum.

Interference mitigation is baked into the waveform itself: the balanced power distribution and strategically placed notches automatically attenuate common jamming tones, thereby reducing the burden on downstream filters. This integrated protection sets the stage for the next level of defense:

Controlled Reception Pattern Antennas (CRPAs). By combining waveform-centric mitigation with CRPA-enabled beamforming and null steering, future receivers can adapt in real time to complex interference and multipath, providing unmatched robustness in the most challenging signal environments.

To learn more, visit www.edgemicrowave.com and follow us on LinkedIn for the latest updates.

FURTHER READING

Langley, R.B., Teunissen, P.J.G., & Montenbruck, O. *Introduction to GNSS*. In *Springer Handbook of Global Navigation Satellite Systems*, Springer, 2017.

Kaplan, E.D., & Hegarty, C.J. (Eds.) *Understanding GPS/GNSS: Principles and Applications* (3rd Edition). Artech House, 2017.

J. Sanz Subirana, J.M. Juan Zornoza and M. HernándezPajares, *GNSS Data Processing, Volume I: Fundamentals and Algorithms. ESA TM-23/1*. ISBN 978-92-9221-886-7. European Space Agency. May 2013.

Flores, A. *NAVSTAR GPS Space Segment/Navigation User Interfaces*. 2021.
https://www.gps.gov/technical/icwg/IS-GPS-200M.pdf

European GNSS Agency, *Galileo Open Service – Signal-in-space interface control document (OS SIS ICD) – Issue 2.1, Publications Office of the European Union, 2023,* ***https://data.europa.eu/doi/10.2878/39727***

Daniel Pascual. *danipascual/GNSS-matlab (https://github.com/danipascual/GNSS-matlab)*, GitHub, 2025. Retrieved May 9, 2025.